Simultaneous Inversion of Pre-stack Seismic Data

Daniel P. Hampson[1], Brian H. Russell[1] and Brad Bankhead[2]

[1]Hampson-Russell Software Ltd,

[2]VeritasDGC

Summary

We present a new approach to the simultaneous pre-stack inversion of *PP* and, optionally, *PS* angle gathers for the estimation of P-impedance, S-impedance and density. Our algorithm is based on three assumptions. The first is that the linearized approximation for reflectivity holds. The second is that *PP* and *PS* reflectivity as a function of angle can be given by the Aki-Richards equations (Aki and Richards, 2002). The third is that there is a linear relationship between the logarithm of P-impedance and both S-impedance and density. Given these three assumptions, we show how a final estimate of P-impedance, S-impedance and density can be found by perturbing an initial P-impedance model. After a description of the algorithm, we then apply our method to both model and real data sets.

Introduction

The goal of pre-stack seismic inversion is to obtain reliable estimates of P-wave velocity (V_P), S-wave velocity (V_S), and density (ρ) from which to predict the fluid and lithology properties of the subsurface of the earth. This problem has been discussed by several authors. Simmons and Backus (1996) invert for linearized P-reflectivity (R_P), S-reflectivity (R_S) and density reflectivity (R_D), where

$$R_P = \frac{1}{2}\left[\frac{\Delta V_P}{V_P} + \frac{\Delta \rho}{\rho}\right], \tag{1}$$

$$R_S = \frac{1}{2}\left[\frac{\Delta V_S}{V_S} + \frac{\Delta \rho}{\rho}\right], \tag{2}$$

$$R_D = \frac{\Delta \rho}{\rho}. \tag{3}$$

Simmons and Backus (1996) also make three other assumptions: that the reflectivity terms given in equations (1) through (3) can be estimated from the angle dependent reflectivity $R_{PP}(\theta)$ by the Aki-Richards linearized approximation (Aki and Richards, 2002, Richards and Frasier, 1976), that ρ and V_P are related by Gardner's relationship (Gardner et al. 1974), given by

$$\frac{\Delta \rho}{\rho} = \frac{1}{4}\frac{\Delta V_P}{V_P}, \tag{4}$$

and that V_S and V_P are related by Castagna's equation (Castagna et al., 1985), given by

(5)

The authors then use a linearized inversion approach to solve for the reflectivity terms given in equations (1) through (3).

Buland and Omre (2003) use a similar approach which they call Bayesian linearized AVO inversion. Unlike Simmons and Backus (1996), their method is parameterized by the three terms $\Delta V_P / V_P$, $\Delta V_S / V_S$, and $\Delta \rho / \rho$, again using the Aki-Richards approximation. The authors also use the small reflectivity approximation to relate these parameter changes to the original parameter itself. That is, for changes in P-wave velocity they write

, (6)

where ln represents the natural logarithm. Similar terms are given for changes in both S-wave velocity and density. This logarithmic approximation allows Buland and Omre (2003) to invert for velocity and density, rather than reflectivity, as in the case of Simmons and Backus (1996). Unlike Simmons and Backus (1996), however, Buland and Omre (2003) do not build in any relationship between P and S-wave velocity, and P-wave velocity and density.

In the present study, we extend the work of both Simmons and Backus (2003) and Buland and Omre (1996), and build a new approach that allows us to invert directly for P-impedance ($Z_P=\rho V_P$), S-impedance ($Z_S=\rho V_S$), and density through a small reflectivity approximation similar to that of Buland and Omre (2003), and using constraints similar to those used by Simmons and Backus (1996). It is also our goal to extend an earlier post-stack impedance inversion method (Russell and Hampson, 1991) so that this method can be seen as a generalization to pre-stack inversion.

Post-stack Inversion For P-impedance

We will first review the principles of model-based post-stack inversion (Russell and Hampson, 1991). First, by combining equations (1) and (6), we can show that the small reflectivity approximation for the P-wave reflectivity is given by

, (7)

where *i* represents the interface between layers *i* and *i+1*. If we consider an *N* sample reflectivity, equation (7) can be written in matrix form as

$$\begin{bmatrix} R_{P1} \\ R_{P2} \\ \vdots \\ R_{PN} \end{bmatrix} = \frac{1}{2}\begin{bmatrix} -1 & 1 & 0 & \cdots \\ 0 & -1 & 1 & \ddots \\ 0 & 0 & -1 & \ddots \\ \vdots & \ddots & \ddots & \ddots \end{bmatrix}\begin{bmatrix} L_{P1} \\ L_{P2} \\ \vdots \\ L_{PN} \end{bmatrix}, \qquad (8)$$

where $L_{Pi} = \ln(Z_{Pi})$. Next, if we represent the seismic trace as the convolution of the seismic wavelet with the earth's reflectivity, we can write the result in matrix form as

$$\begin{bmatrix} T_1 \\ T_2 \\ \vdots \\ T_N \end{bmatrix} = \begin{bmatrix} w_1 & 0 & 0 & \cdots \\ w_2 & w_1 & 0 & \ddots \\ w_3 & w_2 & w_1 & \ddots \\ \vdots & \ddots & \ddots & \ddots \end{bmatrix}\begin{bmatrix} R_{P1} \\ R_{P2} \\ \vdots \\ R_{PN} \end{bmatrix}, \qquad (9)$$

where T_i represents the i^{th} sample of the seismic trace and w_j represents the j^{th} term of an extracted seismic wavelet. Combining equations (8) and (9) gives us the forward model which relates the seismic trace to the logarithm of P-impedance:

$$T = (1/2)WDL_P, \qquad (10)$$

where W is the wavelet matrix given in equation (9) and D is the derivative matrix given in equation (8). If equation (10) is inverted using a standard matrix inversion technique to give an estmate of L_P from a knowledge of T and W, there are two problems. First, the matrix inversion is both costly and potentially unstable. More importantly, a matrix inversion will not recover the low frequency component of the impedance. An alternate strategy, and the one adopted in our implementation of equation (10), is to build an initial guess impedance model and then iterate towards a solution using the conjugate gradient method.

Post-stack Inversion For P-impedance

We can now extend the theory to the pre-stack inversion case. The Aki-Richards equation was re-expressed by Fatti et al. (1994) as

$$R_{PP}(\theta) = c_1 R_P + c_2 R_S + c_3 R_D, \qquad (11)$$

where , $c_2 = -8\gamma^2 \tan^2\theta$, $\gamma = V_S/V_P$, and , and the three reflectivity terms are as given by equations (1) through (3).

For a given angle trace $T(\theta)$ we can therefore extend the zero offset (or angle) trace given in equation (10) by combining it with equation (11) to get

$$T(\theta) = (1/2)c_1 W(\theta)DL_P + (1/2)c_2 W(\theta)DL_S + W(\theta)c_3 DL_D \qquad (12)$$

where $L_S = \ln(Z_S)$ and $L_D = \ln(\rho)$. Note that the wavelet is now dependent on angle. Equation (12) could be used for inversion, except that it ignores the fact that there is a relationship between L_P and L_S and between L_P and L_D.

Because we are dealing with impedance rather than velocity, and have taken logarithms, our relationships are different than those given by Simmons and Backus (1996) and are given by

$$\ln(Z_S) = k\ln(Z_P) + k_c + \Delta L_S, \qquad (13)$$

and

$$\ln(Z_D) = m\ln(Z_P) + m_c + \Delta L_D. \qquad (14)$$

That is, we are looking for deviations away from a linear fit in logarithmic space. This is illustrated in Figure 1.

Combining equations (12) through (14), we get

$$T(\theta) = \tilde{c}_1 W(\theta)DL_P + \tilde{c}_2 W(\theta)D\Delta L_S + W(\theta)c_3 D\Delta L_D, \qquad (15)$$

where $\tilde{c}_1 = (1/2)c_1 + (1/2)kc_2 + mc_3$ and .

Equation (15) can be implemented in matrix form as

$$\begin{bmatrix} T(\theta_1) \\ T(\theta_2) \\ \vdots \\ T(\theta_N) \end{bmatrix} = \begin{bmatrix} \tilde{c}_1(\theta_1)W(\theta_1)D & \tilde{c}_2(\theta_1)W(\theta_1)D & c_3(\theta_1)W(\theta_1)D \\ \tilde{c}_1(\theta_2)W(\theta_2)D & \tilde{c}_2(\theta_2)W(\theta_2)D & c_3(\theta_2)W(\theta_2)D \\ \tilde{c}_1(\theta_N)W(\theta_N)D & \tilde{c}_2(\theta_N)W(\theta_N)D & c_3(\theta_N)W(\theta_N)D \end{bmatrix}\begin{bmatrix} L_P \\ \Delta L_S \\ \Delta L_D \end{bmatrix} \qquad (16)$$

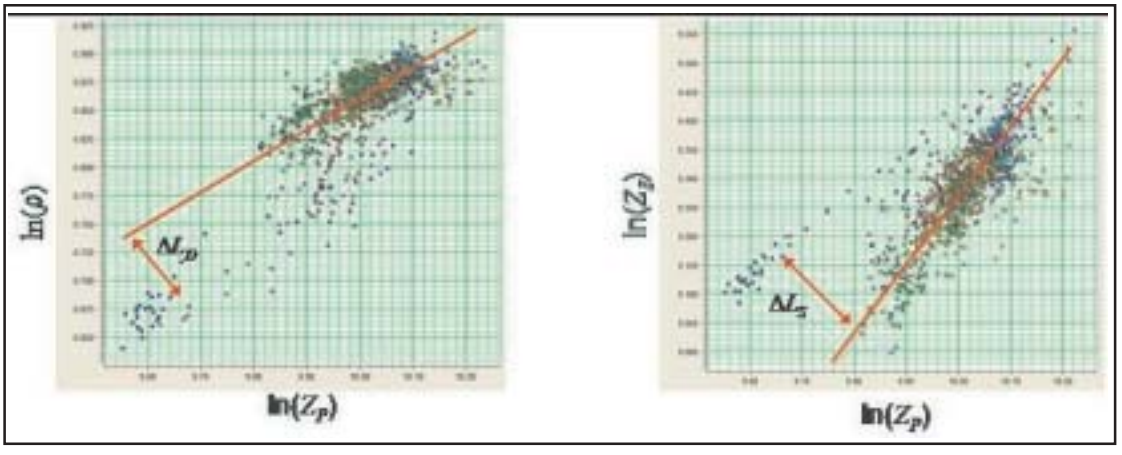

Fig. 1: Crossplots of (a) $\ln(Z_D)$ vs $\ln(Z_P)$ and (b) $\ln(Z_S)$ vs $\ln(Z_P)$ where, in both cases, a best straight line fit has been added. The deviations away from this straight line, ΔL_D and ΔL_S, are the desired fluid anomalies.

If equation (16) is solved by matrix inversion methods, we again run into the problem that the low frequency content cannot be resolved. A practical approach is to initialize the solution to $[L_P \quad \Delta L_S \quad \Delta L_D]^T = [\ln(Z_{P0}) \quad 0 \quad 0]^T$, where Z_{P0} is the initial impedance model, and then to iterate towards a solution using the conjugate gradient method.

In the last section, we will show how to extend the theory in equations (15) and (16) by including *PS* angle gathers as well as *PP* angle gathers.

Model And Real Data Examples

We will now apply this method to both a model and real data example. Figure 2(a) shows the well log curves for a gas sand on the left (in blue), with the initial guess curves (in red) set to be extremely smooth so as not to bias the solution. On the right are the model, the input computed gather from the full well log curves, and the error, which is almost identical to the input. Figure 2(b) then shows the same displays after 20 iterations through the conjugate gradient inversion process. Note that the final estimates of the well log curves match the initial curves quite well for the P-impedance, Z_P, S-impedance, Z_S, and the Poisson's ratio (σ). The density (ρ) shows some "overshoot" above the gas sand (at 3450 ms), but agrees with the correct result within the gas sand. The results on the right of Figure 2(b) show that the error is now very small.

Next, we will use Biot-Gassmann substitution to create the equivalent wet model for the sand shown in Figure 2, and again perform inversion.

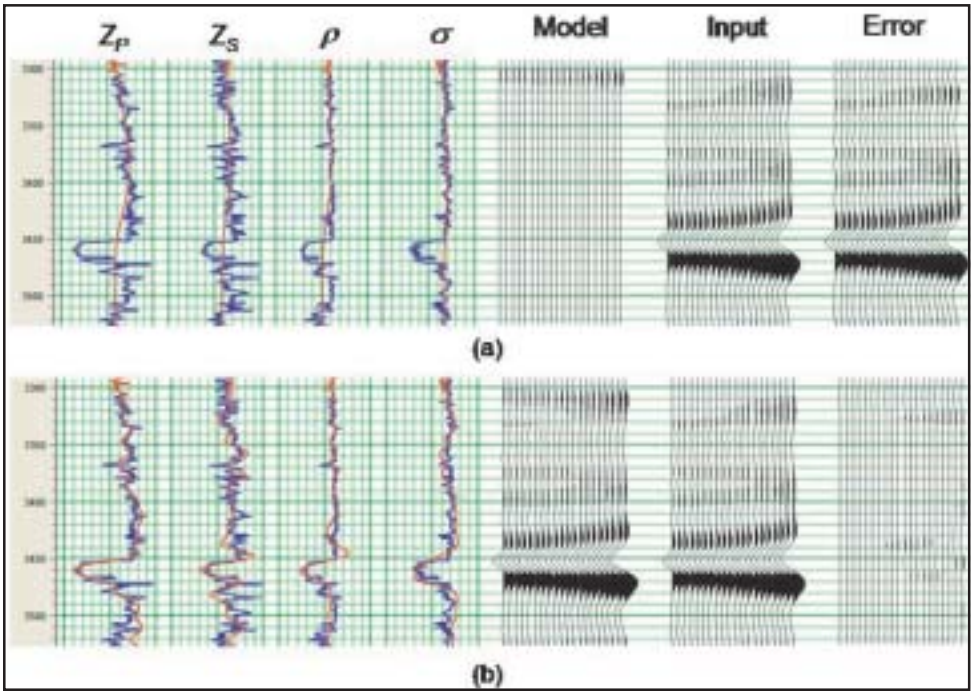

Fig. 2. The results of inverting a gas sand model, where (a) shows the initial model before inversion, and (b) shows the results after inversion.

Figure 3(a) shows the well log curves for the wet sand on the left, with the smooth initial guess curves superimposed in red. On the right are the model from the initial guess, the input modeled gather from the full well log curves, and the error. Figure 3(b) then shows the same displays after 20 iterations through the conjugate gradient inversion process. As in the gas case, the final estimates of the well log curves match the initial curves quite well, especially for the P-impedance, Z_P, S-impedance, Z_S, and the Poisson's ratio (σ). The density (ρ) shows a much better fit at the wet sand (which is at 3450 ms) than it did at the gas sand in Figure 2.

We will next look at a real data example, consisting of a shallow Cretaceous gas sand from central Alberta. Figure 4 shows the computed V_P/V_S ratio from this dataset, where the anomalous gas sand is encircled by the black ellipse. Notice the drop in V_P/V_S associated with the gas sand.

Figure 5 then shows a comparison between the input gathers over the sand (where a clear AVO Class 3 anomaly is evident), and the computed synthetic gathers using the inverted results.

Extension To Converted Wave Data

We will now discuss how the formulation just derived can be extended to include pre-stack converted-wave seismic (PS data) that have been converted to PP time. To do this, we will use the linearized form of the equation was developed by Aki, Richards, and Frasier (Aki and Richards, 2002, Richards and Frasier, 1976). It has been shown by Margrave et al. (2001) that this equation can be written as

$$R_{PS}(\theta,\phi) = c_4 R_S + c_5 R_D, \tag{17}$$

where

$$c_5 = \frac{-\tan\phi}{2\gamma}\left[1 + 2\sin^2\phi - 2\gamma\cos\theta\cos\phi\right]$$

, $\gamma = V_S/V_P$ and . The reflectivity terms R_S and R_D given in equation (17) are identical to the terms those given in equations (2) and (3). Using the small reflectivity approximation, we can re-write equation (17) as:

$$T_{PS}(\theta,\phi) = c_4 W(\phi) DL_S + c_5 W(\phi) DL_D, \tag{18}$$

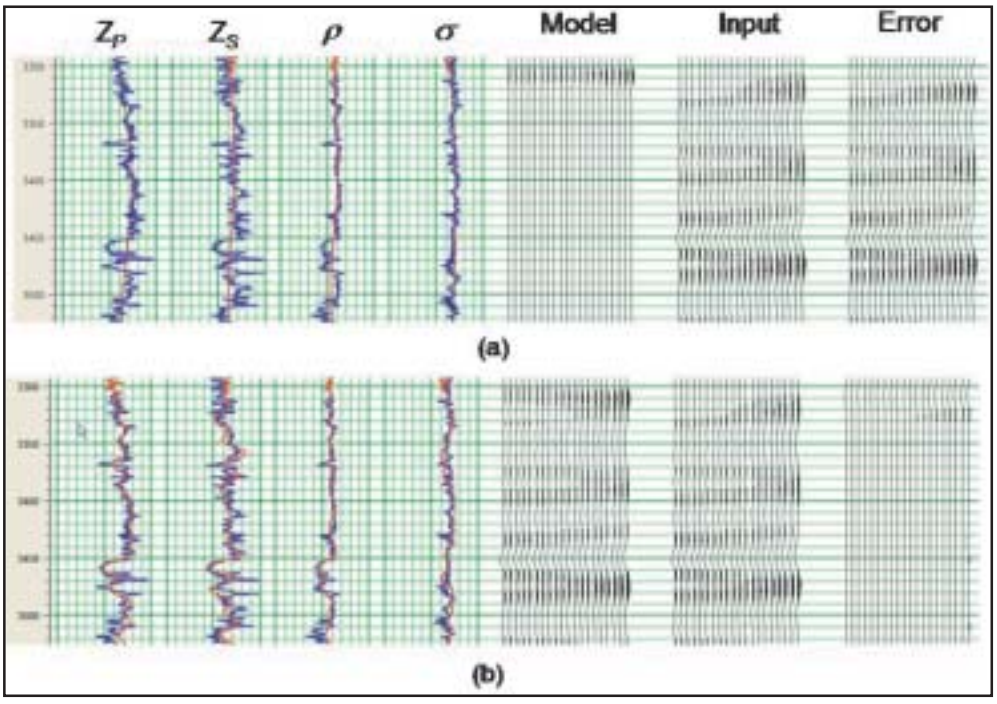

Fig. 3. The results of inverting a wet sand model, where (a) shows the initial model before inversion, and (b) shows the results after inversion.

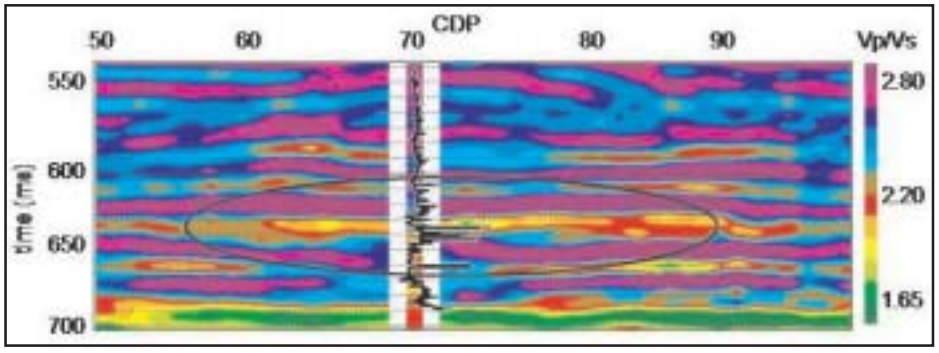

Fig. 4. The inverted V_P/V_S ratio for a shallow gas sand from Alberta, where the elliptical region indicates the anomalous region.

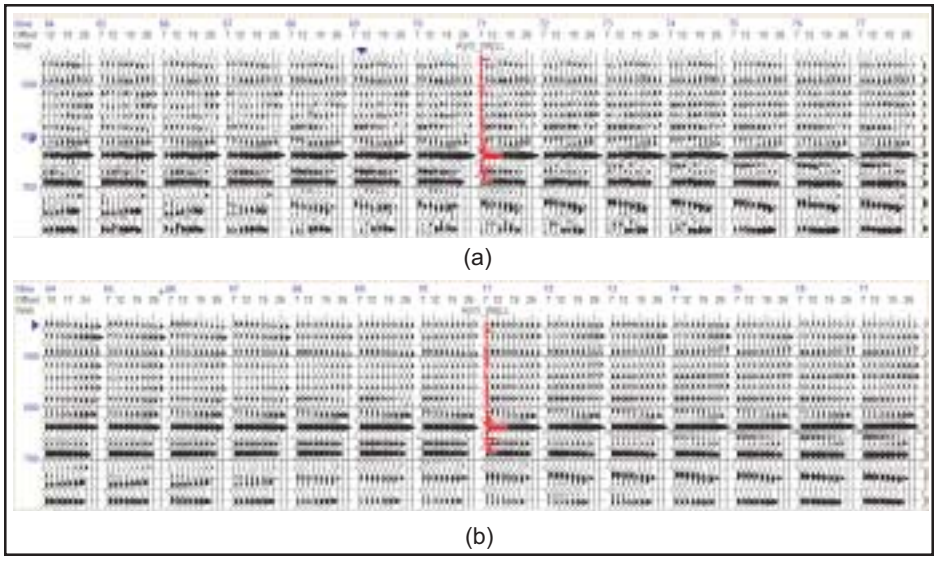

Fig. 5. The CDP gathers over the gas sand anomaly from Fig.4, where (a) shows the input gathers and (b) shows the synthetic gathers after inversion.

Using the relationships between S-impedance, density and P-impedance given in equations (13) and (14), equation (18) can be further re-written as

(19)

where

Note that equation (19) allows us to express a single *PS* angle stack as a function of the same three parameters given in equation (15). Also, equation (19) is given at a single angle ϕ. When we generalize this equation to *M* angle stacks, we can combine this relationship with equation (16) and write the general matrix equation as

$$\begin{bmatrix} T_{PP}(\theta_1) \\ \vdots \\ T_{PP}(\theta_N) \\ T_{PS}(\phi_1) \\ \vdots \\ T_{PS}(\phi_M) \end{bmatrix} = \begin{bmatrix} \tilde{c}_1(\theta_1)W(\theta_1)D & c_2(\theta_1)W(\theta_1)D & c_3(\theta_1)W(\theta_1)D \\ \vdots & \vdots & \vdots \\ \tilde{c}_1(\theta_N)W(\theta_N)D & c_2(\theta_N)W(\theta_N)D & c_3(\theta_N)W(\theta_N)D \\ \tilde{c}_4(\phi_1)W(\phi_1)D & c_4(\phi_1)W(\phi_1)D & c_5(\phi_1)W(\phi_1)D \\ \vdots & \vdots & \vdots \\ \tilde{c}_4(\phi_M)W(\phi_M)D & c_4(\phi_M)W(\phi_M)D & c_5(\phi_M)W(\phi_M)D \end{bmatrix} \begin{bmatrix} L_P \\ \Delta L_S \\ \Delta L_D \end{bmatrix} \quad (20)$$

Equation (20) gives us a general expression for the simultaneous inversion of *N PP* angle stacks and *M PS* angle stacks. Note that we extract a different wavelet for each of the *PS* angle stacks, as was done for each of the *PP* angle stacks.

Conclusions

We have presented a new approach to the simultaneous inversion of pre-stack seismic data which produces estimates of *P*-impedance, *S*-Impedance and density. The method is based on three assumptions: that the linearized approximation for reflectivity holds, that reflectivity as a function of angle can be given by the Aki-Richards equations, and that there is a linear relationship between the logarithm of *P*-impedance and both *S*-impedance and density. Our approach was shown to work well for modelled gas and wet sands and also for a real seismic example which consisted of a shallow Creataceous gas sand from Alberta. Finally, we showed how our method could be extended to include *PS* converted-wave pre-stack data which had been calibrated to *PP* time.

$$\tilde{c}_4(\phi_M)W(\phi_M)D\Delta L_P + c_4W(\phi)D\Delta L_S + c_5W(\phi)D\Delta L_D,$$

References

Aki, K., and Richards, P.G., 2002, Quantitative Seismology, 2nd Edition: W.H. Freeman and Company.

Buland, A. and Omre, H, 2003, Bayesian linearized AVO inversion: Geophysics, **68**, 185-198.

Castagna, J.P., Batzle, M.L., and Eastwood, R.L., 1985, Relationships between compressional-wave and shear-wave velocities in clastic silicate rocks: Geophysics, **50**, 571-581.

Fatti, J., Smith, G., Vail, P., Strauss, P., and Levitt, P., 1994, Detection of gas in sandstone reservoirs using AVO analysis: a 3D Seismic Case History Using the Geostack Technique: Geophysics, **59**, 1362-1376.

Gardner, G.H.F., Gardner, L.W. and Gregory, A.R.,1974, Formation velocity and density - The diagnostic basics for stratigraphic traps: Geophysics, **50,** 2085-2095.

Margrave, G.F., Stewart, R. R. and Larsen, J. A., 2001, Joint *PP* and *PS* seismic inversion: The Leading Edge, **20,** no. 9, 1048-1052.

Richards, P. G. and Frasier, C. W., 1976, Scattering of elastic waves from depth-dependent inhomogeneities: Geophysics, **41,**

Russell, B. and Hampson, D., 1991, A comparison of post-stack seismic inversion methods: Ann. Mtg. Abstracts, Society of Exploration Geophysicists, 876-878.

Simmons, J.L. and Backus, M.M., 1996, Waveform-based AVO inversion and AVO prediction-error: Geophysics, **61**, 1575-1588.